Electronic Supplementary Material (ESI) for Nanoscale.
This journal is © The Royal Society of Chemistry 2020

Supplementary Information for

Mechanical properties of gold nanowires prepared by nanoskiving approach

Zhuo Fang, [a,b] Yanquan Geng,*[a,b] Jiqiang Wang, [a,b] Yongda Yan*[a,b] and Guoxiong Zhang [c]

[a] Key Laboratory of Micro-systems and Micro-structures Manufacturing of Ministry of Education, Harbin Institute of Technology, Harbin, Heilongjiang 150001, China.

[b] Center for Precision Engineering, Harbin Institute of Technology, Harbin, Heilongjiang 150001, China.

[c] College of Precision Instruments and Optoelectronics Engineering, Tianjin University, Tianjin 300072, China.

* To whom correspondence should be addressed: gengyanquan@hit.edu.cn; yanyongda@hit.edu.cn

The current file includes the following:

1. Fabrication of gold NWs using microtome sectioning.

Figure S1 shows the schematic of the fabrication of gold NWs by nanoskiving. First, Silicon wafers are cut into 1×1 cm^2 squares and are cleaned by ultrasonic in DI water and anhydrous ethanol for 10 min, then treated by piranha lotion (98% H_2SO_4: 30% H_2O_2 (v:v)=7:3) at 130 ℃ for 30 min. Finally, the processed silicon wafer is successively put into DI water and anhydrous ethanol to conduct ultrasonic cleaning for 10 min and then blown dry with high-purity nitrogen. Second, the gold film is deposited on the silicon wafer using an electron beam evaporation system (XLT Technology Co. Ltd. China) at a rate of 1 nm/s. Third, the resin and hardener of Epo-fix epoxy (Electron Microscope Sciences, USA) are mixed in 25:3 (w:w) ratios and cured at room temperature for 10-12 h.[1] After peeling off from the substrate, the resin is cut with a razor blade into thin strips (5 mm length × 3 mm width) and the second layer of resin is poured on the surface of the gold film. The epoxy resin block embedded with the gold film is fixed on the sample table of an ultramicrotome (EM UC-7, Leica, Germany). The top surface of the sample is exposed with an ordinary glass knife, and then the epoxy resin around the embedded structure is cut into a convex structure (~500×500 μm). Finally, a diamond knife (1.5 mm Ultra 35°, Diatome, Switzerland) is used for nanoskiving. Using a collection loop (2 mm diameter), the epoxy resin sheet is directionally transferred to the substrate. The resin sheet is then exposed to an oxygen plasma for 30-120 min at 0.24 mbar at 100 W in an oxygen plasma etcher (Zepto, Diener Electronic, Germany) to remove the resin around the nanowire.

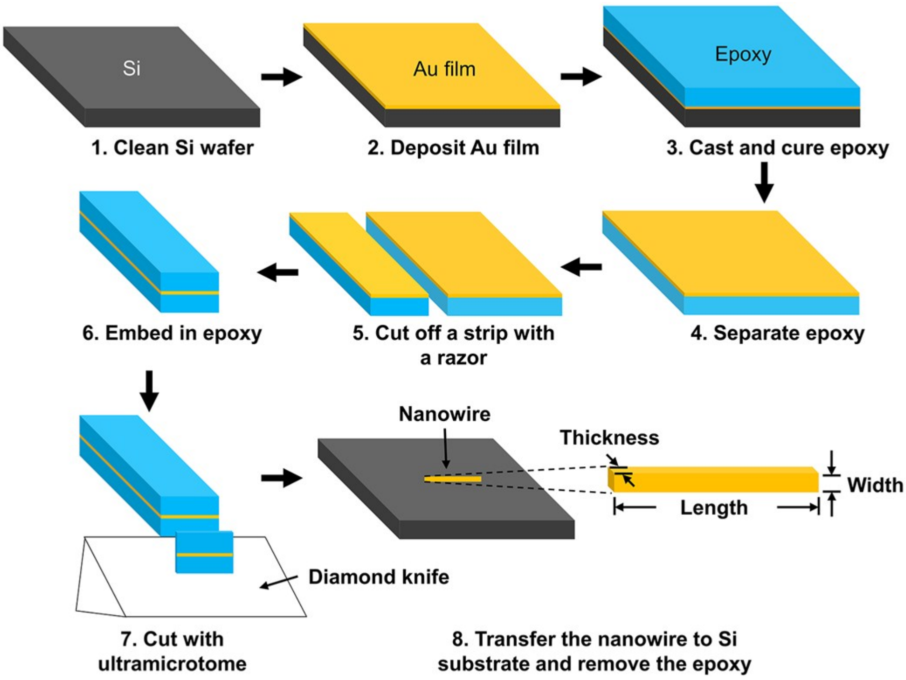

Figure S1. Schematic of the fabrication of gold NWs by nanoskiving.

2. Characterization of as-deposited Au film

The SEM image of the Au film (Figure S2) shows that the film surface is uniform with an average grain size of 25.0±10.4 nm. The complete and small particle size indicates that the synthesized Au film has high purity.

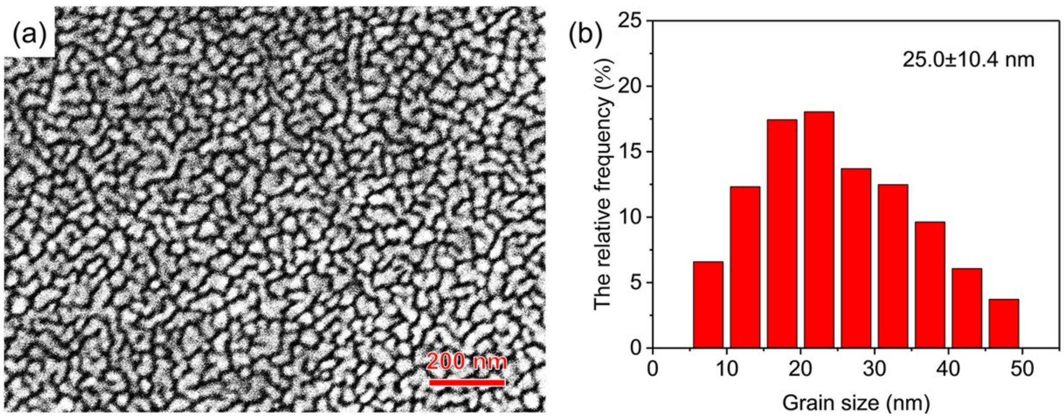

Figure S2. (a) Planar view SEM micrograph of an as-deposited Au film and (b) Statistical distribution of the grain size.

XRD spectra of the Au film reveals that the Au film has different X-ray incident angles, as shown in Figure S3. The crystal face type, in turn, is the 111 and 222 crystal faces, which is consistent with the standard card PDF00-004-0784. It can be clearly determined that the electron beam vapor-deposited Au film is grown along the (111) crystal plane and has no diffraction peaks of other impurity components.

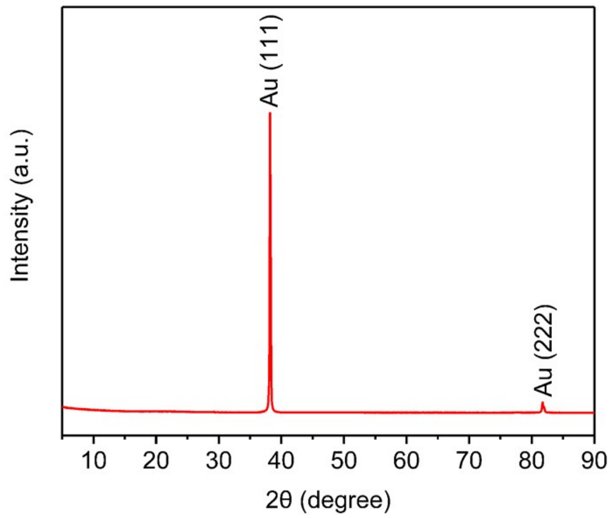

Figure S3. XRD spectra of the Au film on SiO_2.

3. Construction of NW three-point bending test platform

Figure S4 shows the typical transfer and fixation of NWs. It should be noted that the image resolution in the focus ion beam (FIB) is too low to accurately locate the NW when the beam current under 7.7 pA, so all of NWs were fixed under the ion beam of 7.7 pA and 24 pA. Figures S5 (c-d) indicated that the current of 7.7 pA has less damage to the surface of the NWs compare with 24 pA. Thus, we choose this parameter to fix all nanowires in FIB.

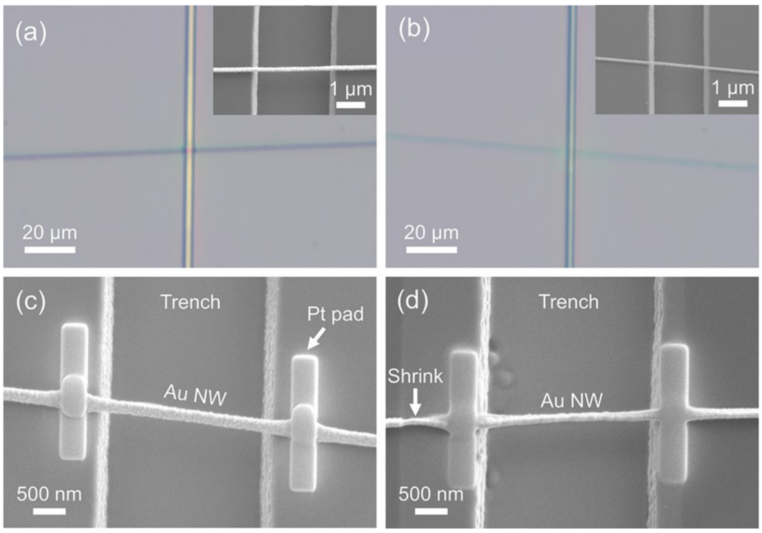

Figure S4. Directional transfer and fixation of NWs. The typical size of NWs is (a) 200 nm high, (b) 30 nm high. Fixed NWs under (c) 7.7 pA (d) 24 pA icon beam current.

4. Young's modulus of Au NWs

Fig. S5 shows the effects of thickness and the surface-to-volume ratio of NWs on Young's modulus with two cutting directions. For both conditions, NWs-a with w=86-193 nm and t=60-228 nm and NWs-b with w=97-170 nm and t=43-295 nm are employed. The red and black solid circles represent the measured results of NWs-a (E_A) and NWs-b (E_B), respectively. The averages are indicated by the dotted red and black lines accordingly.

The average Young's modulus of the NWs-a and NWs-b are 77.2±9.5 GPa and 75.1±11.9 GPa, which agree well with Young's modulus of bulk gold (78 GPa).[2] In Fig. S5a, Young's modulus E_A and E_B of NWs fluctuate irregularly around their averages. There is no obvious correlation between the Young' modulus and their thickness for both cutting directions. Deb Nath et al. have used the molecular dynamics (MD) simulations to reveal that Young's modulus size dependence works only when the diameter of the gold nanowire is less than 30nm.[3] Therefore, the surface relaxation would not be dominant in the range of nanowires cross-section sizes we tested, which is much larger than the critical size of 30 nm.[4-6]

Fig. S5b shows there is no significant difference for Young's modulus of Au NWs with perpendicular and parallel cutting directions while their surface-to-volume ratio varies from 0.019 to 0.054 nm^{-1} and 0.020 to 0.066 nm^{-1}, respectively. Deng et al. have found the elastic modulus does not change in different twin boundary spacing (TBS) by MD simulations.[7] Wu et al. have compared fivefold twinned Ag nanowires with or without annealing and found the annealing process resulting in eliminating twin boundaries in NWs could not affect Young's modulus.[8] These reports have shown that the TBs is also not the main factor determining Young's modulus of NWs.

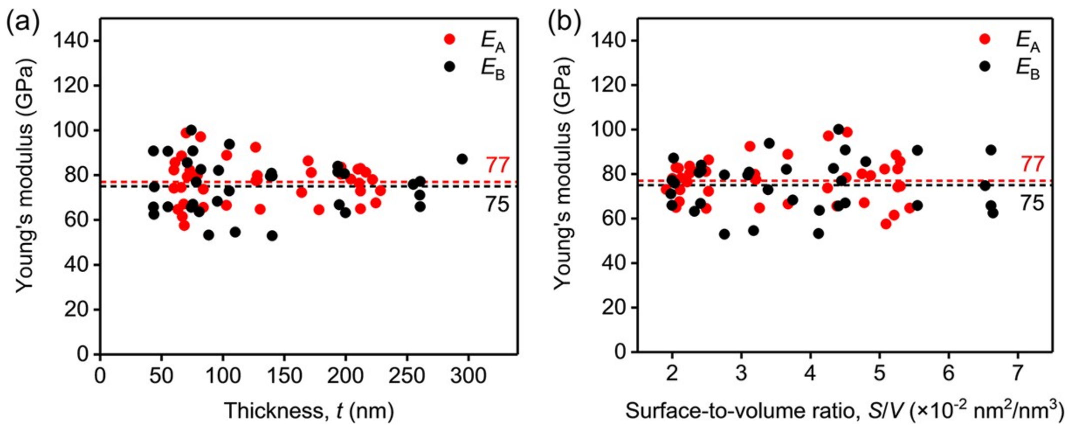

Figure S5. Effects of the (a) thickness and (b) surface-to-volume ratio of NWs on Young's modulus.

5. Measurement error analysis

The major sources of error in our measurements to be: (i) uncertainties in the nanowires width, thickness and suspend length as the nanowire width and height vary slightly in the axial direction (ii) errors in measurement the deflection of AFM cantilever and nonlinear deflection of nanowires and (iii) uncertainties in calibrations of AFM scanner and detector, and cantilever stiffness. Among them, the most significant factor is the width and thickness of nanowires because of the high order denominator dependence in the equation of calculating Young's modulus and yield strength, resulting in a 10% error. In addition, due to a large number of randomly distributed defects in nanowires, the yield strength is often intrinsically dispersive, which is another major source of the yield strength measurement errors. The errors of the expressions in the text are in the same order of magnitude as previous AFM-based tests.[2, 9-11]

6. References.

[1] Q. Xu, R. M. Rioux, M. D. Dickey and G. M. Whitesides, *Acc. Chem. Res.*, 2008, **41**, 1566-1577.

[2] B. Wu, A. Heidelberg and J. J. Boland, *Nat. Mater.*, 2005, **4**, 525-529.

[3] C. Deng and F. Sansoz, *ACS Nano*, 2009, **3**, 3001-3008.

[4] J. G. Guo and Y. P. Zhao, *Nanotechnology*, 2007, **18**, 295701.

[5] G. Yun and H. S. Park, *Phys. Rev. B*, 2009, **79**, 195421.

[6] Z. J. Wang, C. Liu, Z Li and T. Y. Zhang, *J. Appl. Phys. (Melville, NY, U. S.)*, 2010, **108**, 083506.

[7] C. Deng and F. Sansoz, *Nano Lett.*, 2009, **9**, 1517-1522.

[8] B. Wu, A. Heidelberg, J. J. Boland, J. E. Sader, X. Sun and Y. Li, *Nano Lett.*, 2006, **6**, 468-472.

[9] Y. Gao, S. Q. Shi and T. Y. Zhang, *Nanoscale*, 2017, **9**, 6033-6040.

[10] B. Wu, A. Heidelberg, J. J. Boland, J. E. Sader, X. Sun and Y. Li, *Nano Lett.*, 2006, **6**, 468-472.

[11] M. Humar, D. Arcon, P. Umek, M. Skarabot, I. Musevie and G. Bregar, *Nanotechnology*, 2006, **17**, 3869.